Threonine-509 Is a Determinant of Apparent Affinity for Both Substrate and Cations in the Human Na^+/Dicarboxylate Cotransporter†

Jittima Weerachayaphorn and Ana M. Pajor*

Department of Biochemistry and Molecular Biology, University of Texas Medical Branch, Galveston, Texas 77555-0645

Received July 18, 2007; Revised Manuscript Received October 9, 2007

ABSTRACT: The Na^+/dicarboxylate cotransporter (NaDC1) is involved in the absorption of citric acid cycle intermediates from the lumen of the renal proximal tubule and small intestine. The NaDC1 orthologues from human (h) and rabbit (rb) exhibit differences in citrate and cation transport properties. The citrate K_m and sodium K_{Na} values are much larger in human than rabbit NaDC1. Our previous study showed that transmembrane helices (TM) 7, 10, and 11 and associated loop regions contain the amino acids that are important in determining the differences in apparent citrate affinity, whereas TM10 and 11 determine differences in apparent sodium affinity. Chimera R10 (hNaDC1 with a substitution of TM10 and associated loop from rbNaDC1) contains only four amino acid differences between rb and hNaDC1. This chimera has similar apparent affinity for succinate and sodium as the wild-type rbNaDC1, and an intermediate K_m for citrate. To identify individual residues in the TM10 region that determine functional differences between rb and hNaDC1, four mutants were made in which the rabbit sequence was substituted for that of the hNaDC1. Mutants with a serine or threonine at position 509 (or 512 in rbNaDC1) in TM10 have partial changes in K_m for citrate and succinate but larger changes in apparent affinity for cations and substrate specificity for four-carbon dicarboxylates. The results show that the serine or threonine at position 509 (h) or 512 (rb) is the most important determinant of functional differences in apparent affinity for substrate and cations. Furthermore, the results suggest that the cation and substrate binding sites are located in close proximity to one another in NaDC1.

The Na^+/dicarboxylate cotransporter, NaDC1, located on the apical membrane of the epithelial cells of the renal proximal tubule and small intestine, transports citric acid cycle intermediates (*1*). These substrates include succinate, α-ketoglutarate, and citrate, important energy sources for the kidney. Citrate, for example, provides 10−15% of the fuel for renal oxidative metabolism (*2*). Furthermore, the transport of citrate by the renal proximal tubule helps to regulate urinary citrate concentrations. Low concentrations of citrate in the urine are associated with increased risk of kidney stone formation; calcium chelation by citrate normally prevents the precipitation of calcium salts (*3*). NaDC1 also participates in the secretion of a variety of endogenous and exogenous organic anions by providing dicarboxylate substrates for the organic anion exchangers (*4*). NaDC1 belongs to the SLC13 gene family that includes sodium-coupled transporters for dicarboxylates, citrate, and inorganic sulfate.

Several orthologues of NaDC1 have been identified. The NaDC1 transporters from rabbit (rb) and human (h) are 78% identical in amino acid sequence, but they exhibit functional differences (*5*). For instance, the K_m for citrate and K_{Na} for sodium are larger in hNaDC1[1] than in rbNaDC1. The transporters also differ in their sensitivity to inhibition by lithium, which competes with sodium at one of the cation binding sites (*6*, *7*); the hNaDC1 is insensitive to inhibition by lithium (*8*). In a previous study, we found that interactions between transmembrane helices (TM) 7, 10, and 11 contribute to the differences in apparent citrate affinities between human and rabbit NaDC1 (*9*). The differences in sodium affinities between the human and rabbit Na^+/dicarboxylate cotransporters are determined primarily by residues in TM10 and 11, and the difference in lithium sensitivity is determined by TM11.

The purpose of the present study was to identify individual amino acids in the TM 10 region of NaDC1 responsible for differences in substrate and sodium affinity. TM10 and the attached intracellular loop contains four amino acid differences between hNaDC1 and rbNaDC1. Mutant transporters were made containing the amino acid sequence from rbNaDC1 in the hNaDC1 background, and a reverse mutant in the rbNaDC1 background, rbS512T. The results show that a serine or threonine at position 509 (or 512 in rbNaDC1) in TM10 partially determines differences in K_m for citrate and succinate but is sufficient to confer apparent affinity for cations and substrate specificity for four-carbon dicarboxylates. The results are consistent with substrate and cation binding sites in NaDC1 located in close proximity to one another.

EXPERIMENTAL PROCEDURES

Chimeric and Mutant Transporters. The chimeric transporter R10 is based on hNaDC1 with amino acids 485−539

† This work was supported by National Institutes of Health Grant DK46269.

* To whom correspondence should be addressed. Tel: 409-772-3434; fax: 409-772-1374; e-mail: ampajor@utmb.edu.

[1] Abbreviations: rbNaDC1, rabbit Na^+/dicarboxylate cotransporter 1; hNaDC1, human Na^+/dicarboxylate cotransporter 1; R10 chimera, hNaDC1 with TM10 and loop from rbNaDC1; TM, transmembrane helix.

10.1021/bi701417h CCC: $40.75
Published on Web 12/28/2007

replaced with the equivalent amino acids (488−541) from rbNaDC1, consisting of TM10 and associated loop (*9*). The R10 chimera, previously constructed in pSPORT1 plasmid, was subcloned into the pcDNA3.1 (Invitrogen) mammalian expression plasmid, for expression in COS-7 cells. Mutants in this study were generated using the QuikChange site-directed mutagenesis kit (Stratagene) according to the manufacturer's instructions. The mutant transporters are named using the single-letter amino acid code followed by the number of the position that was mutated. The second letter following the sequence number shows the amino acid substituted at that position. The prefix denotes the parental transporter, either rabbit (rb) or human (h) NaDC1. Mutants were verified by sequencing at the Protein Chemistry Laboratory of the University of Texas Medical Branch.

COS-7 Cell Culture. The SV-40 transformed monkey kidney cell line, COS-7, was obtained from the American Type Culture Collection (Rockville, MD) and cultured in DMEM with 4.5 g/L glucose (GIBCO-Invitrogen) supplemented with 10% heat-inactivated fetal calf serum (Hyclone), 100 units/mL penicillin G, and 100 μg/mL streptomycin. Cells were maintained at 37 °C in an atmosphere of 5% CO_2. Cells were plated at a density of 1.2×10^5 cells/well in 24-well plates coated with 5 μg/cm^2 rat-tail collagen I (BD Bioscience-Clontech) for transport assays, or 6-well collagen-coated plates at a density of 3×10^5 cells/well for biotinylation reactions. Twenty-four hours after seeding, cells were transiently transfected with 1.8 μL of FuGENE 6 (Roche Applied Science) and 0.6 μg of plasmid DNA (9:3 ratio, 24-well plates), or with 3 μL of FuGENE 6 and 1 μg of plasmid (3:1 ratio, 6-well plates) (*10*).

Transport Assays. The transport of [^{14}C]succinate (40 mCi/mmol, Moravek) or [^{14}C]citrate (55 mCi/mmol, American Radiolabeled Chemical Inc.) was conducted 48 h after transfections, as described previously (*10*). Each well was washed twice with 1 mL of sodium buffer containing 120 mM NaCl, 5 mM KCl, 1.2 mM $MgSO_4$, 1.2 mM $CaCl_2$, 5 mM D-glucose, 25 mM HEPES, pH adjusted to 7.4 with 1 M Tris. Transport was initiated by incubating the cells 5 min with 250 μL of sodium buffer containing [^{14}C]succinate or [^{14}C]citrate. The surface radioactivity was removed with four washes of 1 mL of sodium buffer. Each well of cells was dissolved in 250 μL of OptiPhase Supermix (Wallac/Perkin-Elmer) scintillation cocktail for 60 min. The plates were then sealed with plastic covers and counted directly in a Microbeta Trilux 1450 plate scintillation counter (Wallac/Perkin-Elmer). The uptake rates were corrected for background counts in control cells transfected with pcDNA3.1 plasmid alone.

In kinetic experiments, 5 min uptakes were measured with increasing concentrations of non-radiolabeled succinate and constant [^{3}H]succinate (50 000 mCi/mmol, ViTrax). [^{3}H]-Succinate was used for increased specific activity at the higher substrate concentrations. Citrate kinetics were measured using a combination of [^{14}C]citrate and non-radioactive citrate. Kinetic constants were calculated by nonlinear regression to the Michaelis−Menten equation using SigmaPlot 2000 software (Jandel Scientific). In sodium activation experiments, the rate of [^{14}C]succinate transport was measured in transport buffer containing sodium concentrations between 0 and 120 mM, with NaCl replaced isoosmotically by choline chloride. Kinetic constants were calculated by nonlinear regression to the Hill equation,

$$v = V_{max}[Na^+]^{n_H}/(K_{Na} + [Na^+])^{n_H}$$

where v is the initial rate uptake, V_{max} is the maximum rate at saturating sodium concentration, $[Na^+]$ is the sodium concentration, K_{Na} is the sodium concentration that produces 1/2 V_{max}, and n_H is the Hill coefficient.

Cell Surface Biotinylation. COS-7 cells were plated in 6-well plates and transfected with 1 μg of plasmid DNA. Cell surface protein expression of NaDC1 and mutants was determined using a membrane impermeant biotin reagent, Sulfo-NHS-LC-biotin (Pierce), and the biotinylated proteins were precipitated using ImmunoPure immobilized streptavidin beads (Pierce), as described previously (*10*). The biotinylated proteins were eluted and separated by SDS-polyacrylamide gel electrophoresis (SDS-PAGE) using a 7.5% Tricine gel and then electrophoretically transferred to nitrocellulose membranes (0.45 μM; Schleicher & Schuell). The blots were blocked, washed, and incubated overnight at 4 °C with anti-rabbit NaDC1 antiserum (diluted 1:1,000 in phosphate-buffered saline containing 0.5% non-fat dried milk and 0.05% TWEEN 20), followed by 1 h incubation at room temperature with 2° antibody (horseradish peroxidase-coupled donkey anti-rabbit Ig (Amersham), diluted 1:5000). Immunoreactive protein signals were detected using the Supersignal West Pico chemiluminescent substrate kit (Pierce). Images were acquired with a Kodak Image Station 440CF imager (Eastman Kodak Co.). The molecular mass was estimated by comparison with chemiluminescent protein size standards (MagicMark Western XP; Invitrogen). The intensity of protein bands was analyzed using Image 1D analysis software.

Data Analysis. Data are presented as means ± SEM (or range if $N = 2$) and N values represent sample size. Differences between groups were determined using Student's *t*-test or one-way analysis of variance followed by Dunnett's test (SigmaStat program, Jandel Scientific). Differences with $p < 0.05$ were considered statistically significant.

RESULTS

Mutants in TM10 and Loop. Our previous study showed that the R10 chimera, hNaDC1 with a substitution of transmembrane helix (TM) 10 and associated loop from rbNaDC1, contains amino acids that are important in determining some of the differences in citrate and sodium affinity (*9*). This region has only four amino acid differences between the human and rabbit NaDC1 (Figure 1). To identify the amino acid responsible for functional differences between the rabbit and human orthologues, we replaced amino acids in hNaDC1 one at a time with the corresponding amino acid from rbNaDC1. The four mutants created were as follows: hT509S in the putative transmembrane helix, and hD530G, hK532R, and hL534S in the intracellular loop between TM 10 and 11 (the prefix h denotes the hNaDC1 parental transporter).

Protein Expression of Mutants. The abundance of mutant proteins on the plasma membrane of transfected COS-7 cells was examined by biotinylation with the membrane impermeant reagent, Sulfo-NHS-LC-biotin, followed by Western blotting. Figure 2A shows single representative blots for human and rabbit mutants compared with the parental transporters, either hNaDC1 or rbNaDC1. The blots were

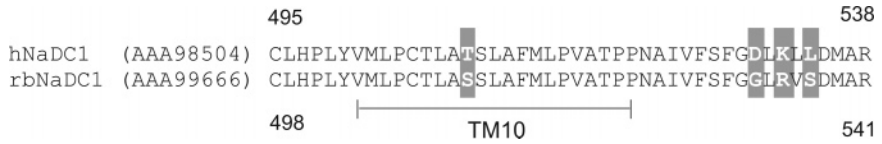

FIGURE 1: Sequence alignment of amino acids 495−538 of human NaDC1 with amino acids 498−541 of rabbit NaDC1. The four amino acid differences are highlighted in gray, and the amino acids that are predicted to form TM10 are underlined. Genbank accession numbers of the sequences are in parentheses.

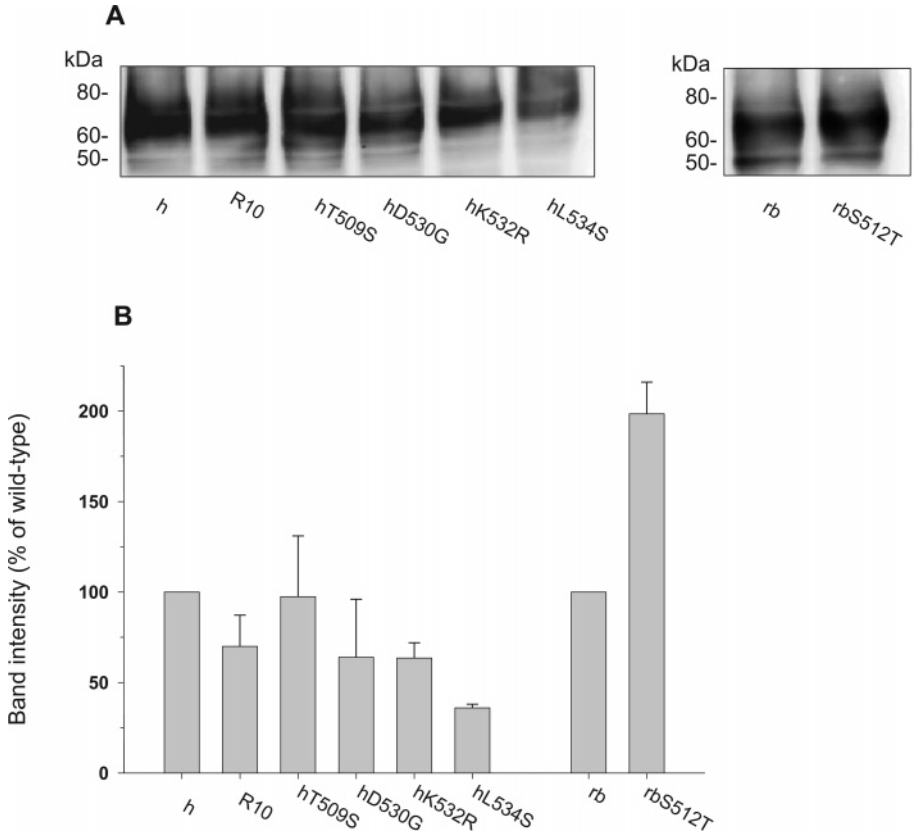

FIGURE 2: Cell surface protein expression of mutants. (A) COS-7 cells expressing wild-type and mutant transporters were treated with Sulfo-NHS-LC-biotin as described in Experimental Procedures. Western blots of biotinylated proteins were probed with anti-NaDC1 antibodies (1:1000 dilution). The positions of the molecular mass standards (MagicMark XP) are indicated on the left. Each blot includes an internal control of the parental transporter, either hNaDC1 (h) or rbNaDC1 (rb). (B) Western blots such as those shown in (A) were quantitated and expressed as a percentage of the parental transporter intensity from the same blot. The bars represent mean ± range ($N = 2$ blots, separate transfections).

scanned to quantitate the protein expression, and each mutant was expressed as a percentage of the parental protein abundance (Figure 2B). The rbNaDC1 expression was 129 ± 11% ($N = 2$) of that of hNaDC1 (not shown), with the assumption that the antibodies, raised against rbNaDC1, recognize the human and rabbit proteins with similar efficiency. All of the mutants were expressed at the plasma membrane, most with more than 60% of the parental transporter abundance, except for hL534S, which was approximately 35%. The rabbit mutant, rbS512T, was more abundant than the parental. Overall, there was no impairment in protein trafficking or stability of the mutants.

Transport Activity of Mutants. The initial rate of uptake was determined by measuring the time courses of citrate and succinate uptake by rb and hNaDC1 transiently transfected in COS-7 cells. The time courses were linear up to 15 min (data not shown). Therefore, an incubation time of 5 min was chosen for subsequent experiments. We examined transport activity of the mutants by comparing the uptake of 1 mM citrate and 1 mM succinate (Figure 3A). As shown in Figure 3B, the rate of citrate transport expressed as a percentage of succinate transport was 97% in rbNaDC1 and 19% in hNaDC1, consistent with our previous study done with *Xenopus* oocytes (*9*). The R10 chimera exhibited intermediate citrate:succinate transport activity compared with the two parental transporters. The hT509S mutant also had intermediate citrate:succinate transport activity, but it was significantly lower than the R10 chimera. The hD530G, hK532R, and hL534S mutants were not significantly different from the parental hNaDC1.

Succinate and Citrate Kinetics. The rbNaDC1 expressed in COS-7 cells had a mean K_m for citrate of about 270 μM, whereas hNaDC1 had a mean K_m for citrate of about 4000 μM (Table 1). The R10 chimera containing transmembrane helix 10 from rabbit in hNaDC1 background had an intermediate citrate K_m value of about 760 μM, significantly lower than the parental hNaDC1. The results are consistent with our previous study comparing the properties of rb and hNaDC1 expressed in *Xenopus* oocytes, with citrate K_m values of 900 μM (rbNaDC1), 7200 μM (hNaDC1), and 3700

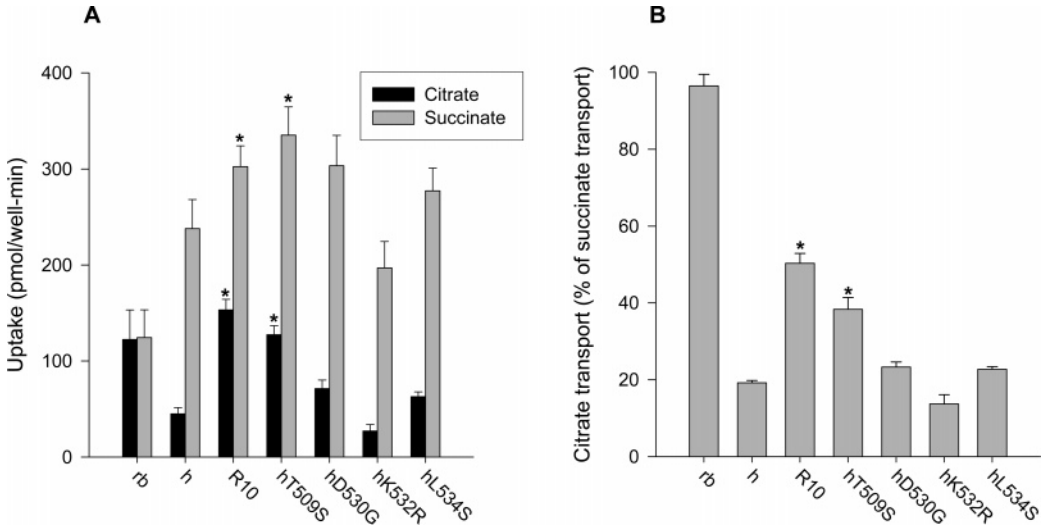

FIGURE 3: Transport activity of NaDC1 mutants. (A) The transport of 1 mM [^{14}C]citrate or 1 mM [^{14}C]succinate was measured for 5 min in sodium containing buffer. (B) The transport of citrate expressed as a percentage of succinate transport, calculated using the data shown in part A. The bars represent mean ± SEM, $N = 3$ experiments. The * denotes significant difference compared with hNaDC1 ($p < 0.05$).

Table 1: Citrate and Succinate Kinetics in Mutants[a]

	citrate kinetics			succinate kinetics		
transporters	K_m (μM)	V_{max} (pmol/well-min)	N	K_m (μM)	V_{max} (pmol/well-min)	N
hNaDC1	3967 ± 377	317 ± 59	3	782 ± 141	188 ± 79	4
R10 chimera	756 ± 112[b]	218 ± 38	4	149 ± 11[b]	378 ± 13	3
hT509S	1325 ± 256[b]	373 ± 176	3	217 ± 19[b]	510 ± 61	3
hD530G	2615 ± 298	527 ± 113	3	836 ± 178	570 ± 37	3
hK532R	3332 ± 284	488 ± 139	3	1041 ± 197	463 ± 127	3
hL534S	2552 ± 691	390 ± 99	3	554 ± 129	452 ± 61	3
hT509S/D530G/L534S	1454 ± 404[b]	552 ± 116	3	138 ± 6[b]	405 ± 171	3
rbNaDC1	274 ± 14	131 ± 16	3	96 ± 12	104 ± 27	3
rbS512T	1791 ± 325[c]	125 ± 12	3	1347 ± 421[c]	246 ± 43	3

[a] The kinetics of citrate and succinate transport were determined in COS-7 cells expressing rbNaDC1, hNaDC1, chimera R10, and mutants. Five minute uptakes were measured. The kinetic values shown are the mean ± SEM. N is sample size. [b] Significant difference compared with the parental hNaDC1 ($p < 0.05$). [c] Significant difference compared with the parental rbNaDC1 ($p < 0.05$) The K_m values for human and rabbit NaDC1 are significantly different from one another.

μM (R10 chimera) (*9*). The succinate K_m values determined in the oocyte expression system were 500 μM (rabbit) and 800 μM (human) (*8*). In the present study, the K_m value for succinate was about 100 μM in rabbit and about 800 μM in hNaDC1. For some reason, the kinetic values for rbNaDC1 are lower when expressed in mammalian cells compared with *Xenopus* oocytes (*11*). The R10 chimera had a succinate K_m of about 150 μM, similar to that of the rabbit NaDC1 although significantly higher.

The most striking effect of single mutations on succinate and citrate kinetics was seen at position 509. The hT509S mutant had a shift in the K_m for both citrate and succinate from the characteristics of hNaDC1 to an intermediate value between h and rbNaDC1 (the single experiments are shown in Figure 4A and B, and the mean of three experiments is in Table 1). The K_m value for citrate in hT509S was significantly higher than that of the R10 chimera, but the K_m value for succinate was similar between hT509S and R10. The hD530G, hL534S, and hK532R mutants had no significant changes in citrate or succinate K_m values. Because the hT509S mutant was different than chimera R10, we further tested the effects of multiple mutations including T509S. The triple mutant (hT509S/D530G/L534S) had no changes in cell surface expression (data not shown) and showed no significant functional differences compared with the hT509S mutant alone (Table 1).

To verify the importance of Thr-509 in determining differences in citrate and succinate affinity, we mutated the serine at the equivalent position in rbNaDC1 (Ser-512) to threonine. The rbS512T mutant exhibited increased K_m values for both citrate and succinate. The K_m for succinate of about 1300 μM was not significantly different from that of hNaDC1, whereas the K_m for citrate of 1800 μM was intermediate between the rabbit and human values (Table 1). Therefore, the kinetic studies confirm that the serine or threonine at position 509 (h) or 512 (rb) is a determinant of citrate and succinate affinity in NaDC1.

Differences in Substrate Specificity Are Also Determined by Amino Acid 509. The rabbit and human NaDC1 transporters also differ in their handling of four or five carbon dicarboxylate substrates, including fumarate, methylsuccinate, and malate (*7*, *8*, *12*). The substrate specificity of the wild-type and mutant transporters was tested by measuring the transport of succinate in the presence of test inhibitors (Figure 5). The inhibition by α-ketoglutarate was relatively low, verifying that the affinity for this substrate is low in both human and rabbit NaDC1. The $K_{0.5}$ for α-ketoglutarate in hNaDC1 expressed in *Xenopus* oocytes is around 16 mM (*12*). The sensitivity of rbNaDC1 to inhibition by succinate,

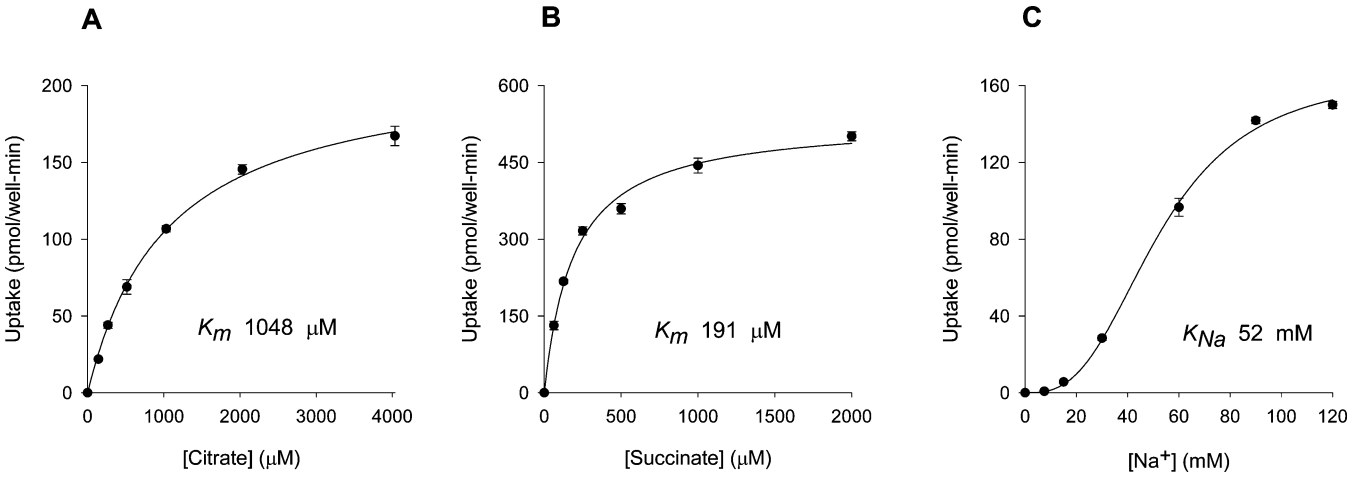

FIGURE 4: Functional properties of the hT509S mutant. (A) Citrate kinetics and (B) succinate kinetics were determined in COS-7 cells expressing the hT509S mutant. The uptake rates of [^{14}C]citrate or [^{3}H]succinate were measured for 5 min. (C) Sodium activation of succinate transport by COS-7 cells expressing the hT509S mutant. Five minute uptakes of 100 μM [^{14}C]succinate were measured in sodium concentrations up to 120 mM NaCl (NaCl was replaced by choline chloride). Each data point shows the mean ± range ($N = 2$) from a single experiment. The results of three separate experiments are shown in Table 1.

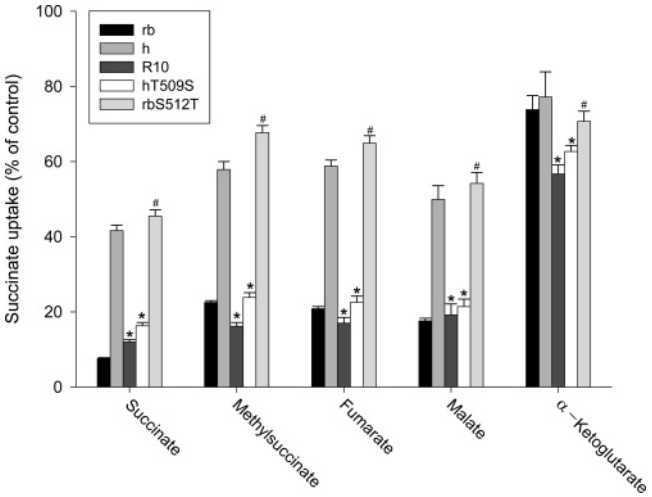

FIGURE 5: Substrate specificity of NaDC1 mutants. Transport of 10 μM [^{14}C]succinate was measured for 5 min in the presence or absence of 1 mM test inhibitors. The transport in the presence of inhibitors is expressed as a percentage of control measured without inhibitors. The bars represent mean ± SEM, $N = 3-4$ experiments. The * denotes significant difference compared with the parental hNaDC1 and the # denotes significant difference compared with the parental rbNaDC1 ($p < 0.05$).

Table 2: Na^+ Activation of Succinate Transport in NaDC1 Mutants[a]

	Na activation		
WT/mutants	K_{Na} (mM)	V_{max} (pmol/well-min)	(n_H)
hNaDC1	112 ± 25	55 ± 16	2.6 ± 0.4
R10 chimera	49 ± 3[b]	163 ± 19	2.6 ± 0.2
hT509S	51 ± 2[b]	153 ± 9	2.9 ± 0.2
rbNaDC1	30 ± 1	65 ± 24	2.5 ± 0.3
rbS512T	46 ± 3[c]	21 ± 2	2.6 ± 0.1

[a] Sodium activation of succinate transport in COS-7 cells expressing the wild-type or mutant NaDC1 transporters. Five minute uptakes of 100 μM [^{14}C]succinate were measured in buffer containing sodium concentrations up to 120 mM. NaCl was replaced by choline chloride. The data represent the mean ± SEM, $N = 3$ experiments. Data were fitted to the Hill equation by nonlinear regression, the Hill coefficient is n_H. [b] Denotes significant difference compared with the parental hNaDC1. [c] Significant difference compared with the parental rbNaDC1 ($p < 0.05$).

methylsuccinate, fumarate, and malate was greater than that of hNaDC1 (Figure 5). The R10 chimera, with TM10 from rbNaDC1 in a hNaDC1 background, had the substrate specificity of rbNaDC1. The single mutation at position 509/512, hT509S and rbS512T, was sufficient to confer the substrate specificity of the donor. These results verify that the serine at position 509/512 is an important determinant of substrate specificity.

Thr-509 Determines Differences in Sodium Affinity. The activation of succinate transport by sodium was measured for wild-type and mutant transporters. There was a sigmoid relationship between sodium concentration and succinate transport rate, with apparent K_{Na} values of 30 mM for rbNaDC1 and 112 mM for hNaDC1 (Table 2), consistent with previous studies (*8*, *9*). The addition of rabbit sequences in the R10 chimera and the hT509S mutant resulted in K_{Na} values that were significantly lower than that of the parental hNaDC1 (Figure 4 and Table 2). The reverse mutation, rbS512T, produced a significant increase in K_{Na} compared with the parental rbNaDC1 transporter, but the effect was quite modest compared with the threonine to serine mutation at position 509 in the human transporter. The Hill coefficient (n_H) remained unchanged for parental transporters and mutants.

DISCUSSION

The present study was based on previous observations that differences in apparent affinity for substrate and cations between the rabbit and human NaDC1 transporters are determined by residues located in transmembrane helices (TM) 7, 10, and 11 (*9*). Chimeras made between rb and hNaDC1 had the apparent citrate affinity of the donor of TM 7, 10, and 11 and associated loops, whereas TM 10 and 11 were sufficient to transfer apparent cation affinity of the donor. The TM 10 region used in the chimera study has only four amino acid differences between the human and rabbit sequences. To identify individual residues in this region that determine the functional differences, four mutants were made with the rabbit sequence substituted for that of the hNaDC1. The major finding of this study is that the residue at position

509 (human) or 512 (rabbit) is critical for determining apparent affinity for both substrate and cations in NaDC1. When position 509/512 is occupied by a serine, as in the rbNaDC1, the apparent affinity for substrates and sodium is higher than when a threonine is found at this position. Furthermore, the results are consistent with cation and substrate binding sites in NaDC1 located in close proximity to one another.

The current secondary structure model of NaDC1 contains 11 TM, with an intracellular amino-terminus and an extracellular N-glycosylated carboxy-terminus (*13*). TM9 and the connecting loop to TM10 form part of the permeation pathway in NaDC1, and this region contains functionally important residues that are alternately accessible and inaccessible to the extracellular medium during the transport cycle (*10*, *14*). Our model places Thr-509 in the TM10 helix and Asp-530, Lys-532, and Leu-534 in the intracellular loop between TM10 and 11 (Figure 1). The relative position of Thr-509/Ser-512 within the middle of the transmembrane helix is consistent with the locations of substrate and cation binding sites within aqueous cavities formed by multiple helices of the known structural models of ion-coupled transport proteins, including the H^+-coupled lactose permease (*15*), Na^+-dependent leucine transporter, $LeuT_{Aa}$ (*16*), and the Na^+-dependent aspartate transporter, Glt_{Ph} (*17*).

The substrate specificity profile can be converted between the rabbit and human phenotypes by the presence of serine or threonine at position 509 (h) or 512 (rb) (see alignment, Figure 1). The same serine or threonine mutation at position 509/512 produces changes in citrate and succinate K_m to values intermediate between the human and rabbit NaDC1. The difference in apparent affinity for citrate or succinate probably requires interaction with additional amino acids, most likely located in TM 7 and 11 based on our previous study (*9*), to completely change the K_m. The amino acid at position 509/512 is also involved in binding other substrates. In a study of mouse NaDC1, we found that serine replacement of the equivalent position at Ala-504 produced a more rabbit-like phenotype with decreased affinity for succinate and adipate, although the reverse mutation in rabbit (rbS512A) was not sufficient to increase affinity for adipate (*18*). The S512C mutant of rbNaDC1 was not expressed on the cell surface, possibly because of protein misfolding (*10*). Similarly, the T509C mutant of hNaDC1 was also not expressed on the cell surface (unpublished results). Cysteine is found at this position in the high affinity NaDC3 transporters.

The transport of dicarboxylates in NaDC1 is a sodium-dependent process that involves an ordered, cooperative binding of three sodium ions followed by substrate (*12*, *19*). An alteration in the Na^+ activation kinetics with an increase in sodium affinity was observed for hT509S, which was similar to chimera R10. Although the single mutation of hNaDC1 was sufficient to convert the K_{Na} almost completely to that of the rabbit, only a partial change in phenotype was seen in the reverse mutant, rbS512T. One possible explanation is that another residue, different in human and rabbit NaDC1, is also involved in determining the difference in apparent cation affinity. In the human, the serine to threonine mutation is compatible with the endogenous second residue, but in the rabbit, the addition of threonine is not sufficient to overcome the properties of the endogenous second residue.

The involvement of a single residue in determining differences in both substrate and cation affinity could be explained by cation and substrate binding sites in close proximity to one another, similar to recent structures of sodium-coupled transporters. For example, in the Na^+/aspartate transporter, Glt_{Ph}, the substrate and cation binding sites are located close together. One residue, Ser-278, interacts with one of the sodium ions through the hydroxyl group and also with the substrate through the backbone nitrogen of the same serine (*20*). In the Na^+/leucine cotransporter, $LeuT_{Aa}$, the substrate itself helps to coordinate one of the sodium ions (*16*). Therefore, a mutation in the substrate binding site could alter cation affinity by either changing the position of the substrate within its binding site or changing the position of residues in the protein that interact with the cation. An alternate possibility is that Thr-509 (hNaDC1) or Ser-512 (rb) is not directly involved in substrate or cation binding but rather is important in holding key residues in place. In the mitochondrial citrate transport protein (CTP), a sodium-independent transporter that is not related in sequence to NaDC1, mutation of Ser-123 to Cys increases the citrate K_m fivefold, although the structural model places this residue near (but not in direct contact with) the substrate (*21*).

Since only the 509/512 residue of TM 10 is different between the human and rabbit NaDC1, the threonine-serine substitutions would not alter the structure of the helix with the exception of the side chain properties at the 509 or 512 position. The hydroxyl group of serine or threonine does not appear to be required for function since the mouse NaDC1 contains alanine at this position, and the S512A mutant of rbNaDC1 does not exhibit any change in functional properties (*18*). Possibly the size or volume of the side chain at this position affects the substrate binding site in NaDC1. In the Na^+/Cl^--glycine transporters, GLYT1 and 2, substrate selectivity is determined by the presence of a glycine or serine in TM 6, and mutants containing the smaller glycine residue can accommodate larger substrates in the binding site (*22*). It should be noted that Thr-509/Ser-512 of NaDC1 determines differences in function. There are likely to be multiple amino acids involved in coordinating each sodium ion and forming the substrate binding site, and these would probably be in common in the human and rabbit Na^+/dicarboxylate cotransporters.

In summary, we have identified Thr-509 (h) or Ser-512 (rb) as a key residue in TM 10 that determines functional differences in apparent affinity for substrate and cations between rabbit and human NaDC1. This residue also determines differences in specificity for dicarboxylate substrates between the two transporters. The results confirm the important role of TM10 in forming part of the substrate and cation binding sites. Since a single residue affects both transport properties, it is possible that NaDC1 resembles other sodium-coupled transporters in having substrate and cation binding sites in close proximity to one another.

ACKNOWLEDGMENT

We thank Aditya Joshi and Kate Randolph for making and testing the T509C mutant of hNaDC1.

REFERENCES

1. Pajor, A. M. (2006) Molecular properties of the SLC13 family of dicarboxylate and sulfate transporters, *Pflugers Arch. 451*, 597−605.
2. Nieth, H., and Schollmeyer, P. (1966) Substrate-utilization of the human kidney, *Nature 209*, 1244−1245.
3. Pak, C. Y. (1991) Etiology and treatment of urolithiasis, *Am. J. Kidney Dis. 18*, 624−637.
4. Wright, S. H., and Dantzler, W. H. (2004) Molecular and cellular physiology of renal organic cation and anion transport, *Physiol. Rev. 84*, 987−1049.
5. Pajor, A. M. (1996) Molecular cloning and functional expression of a sodium-dicarboxylate cotransporter from human kidney, *Am. J. Physiol 270*, F642−F648.
6. Wright, E. M., Wright, S. H., Hirayama, B., and Kippen, I. (1982) Interactions between lithium and renal transport of Krebs cycle intermediates, *Proc. Natl. Acad. Sci. U.S.A. 79*, 7514−7517.
7. Pajor, A. M., Hirayama, B. A., and Loo, D. D. (1998) Sodium and lithium interactions with the Na^+/dicarboxylate cotransporter, *J. Biol. Chem. 273*, 18923−18929.
8. Pajor, A. M., and Sun, N. (1996) Functional differences between rabbit and human Na^+-dicarboxylate cotransporters, NaDC-1 and hNaDC-1, *Am. J. Physiol. 271*, F1093−F1099.
9. Kahn, E. S., and Pajor, A. M. (1999) Determinants of substrate and cation affinities in the Na^+/dicarboxylate cotransporter, *Biochemistry 38*, 6151−6156.
10. Pajor, A. M., and Randolph, K. M. (2005) Conformationally sensitive residues in extracellular loop 5 of the Na^+/dicarboxylate co-transporter, *J. Biol. Chem. 280*, 18728−18735.
11. Weerachayaphorn, J., and Pajor, A. M. (2007) Sodium-dependent extracellular accessibility of Lys-84 in the sodium/dicarboxylate cotransporter, *J. Biol. Chem 282*, 20213−20220.
12. Yao, X., and Pajor, A. M. (2000) The transport properties of the human renal Na^+-dicarboxylate cotransporter under voltage-clamp conditions, *Am. J. Physiol. Renal Physiol. 279*, F54−F64.
13. Zhang, F. F., and Pajor, A. M. (2001) Topology of the Na^+/dicarboxylate cotransporter: the N-terminus and hydrophilic loop 4 are located intracellularly, *Biochim. Biophys. Acta 1511*, 80−89.
14. Pajor, A. M. (2001) Conformationally sensitive residues in transmembrane domain 9 of the Na^+/dicarboxylate co-transporter, *J. Biol. Chem. 276*, 29961−29968.
15. Abramson, J., Smirnova, I., Kasho, V., Verner, G., Kaback, H. R., and Iwata, S. (2003) Structure and mechanism of the lactose permease of *Escherichia coli*, *Science 301*, 610−615.
16. Yamashita, A., Singh, S. K., Kawate, T., Jin, Y., and Gouaux, E. (2005) Crystal structure of a bacterial homologue of Na^+/Cl^--dependent neurotransmitter transporters, *Nature 437*, 215−223.
17. Yernool, D., Boudker, O., Jin, Y., and Gouaux, E. (2004) Structure of a glutamate transporter homologue from *Pyrococcus horikoshii*, *Nature 431*, 811−818.
18. Oshiro, N., and Pajor, A. M. (2006) Ala-504 is a determinant of substrate binding affinity in the mouse Na^+/dicarboxylate cotransporter, *Biochim. Biophys. Acta 1758*, 781−788.
19. Wright, S. H., Hirayama, B., Kaunitz, J. D., Kippen, I., and Wright, E. M. (1983) Kinetics of sodium succinate cotransport across renal brush-border membranes, *J. Biol. Chem. 258*, 5456−5462.
20. Boudker, O., Ryan, R. M., Yernool, D., Shimamoto, K., and Gouaux, E. (2007) Coupling substrate and ion binding to extracellular gate of a sodium-dependent aspartate transporter, *Nature 445*, 387−393.
21. Ma, C., Kotaria, R., Mayor, J. A., Remani, S., Walters, D. E., and Kaplan, R. S. (2005) The yeast mitochondrial citrate transport protein: characterization of transmembrane domain III residue involvement in substrate translocation, *J. Biol. Chem. 280*, 2331−2340.
22. Vandenberg, R. J., Shaddick, K., and Ju, P. (2007) Molecular basis for substrate discrimination by glycine transporters, *J. Biol. Chem. 282*, 14447−14453.

BI701417H